A 3D MR-acquisition scheme for non-rigid bulk motion correction in simultaneous PET-MR

Christoph Kolbitsch[1], Claudia Prieto[1], Charalampos Tsoumpas[1], and Tobias Scheaffter[1]
[1]*Division of Imaging Sciences and Biomedical Engineering, King's College London, London, London, United Kingdom*

INTRODUCTION: In oncology positron emission tomography (PET) is commonly used to detect cancerous tissue and assess the progress of cancer treatment [1]. A partial or complete metabolic response to treatment is defined as a change in standardized uptake values (SUV) of 20% to 50% depending on tumour and study type [2]. Due to long scan times required in PET physiological motion can reduce the obtained image quality and severely impair any quantitative assessments [3]. Simultaneous PET-MR combines metabolic information acquired with PET with high-resolution anatomical MR images [4,5] and has the potential to minimize motion artefacts and improve treatment assessment.

An approach which allows for the automatic detection and correction of bulk motion shifts in PET and MR images (both T1-weighted gradient echo (GRE) and T2-weighted turbo spine echo (TSE) images) has recently been proposed [6]. Here, we present a detailed analysis of the accuracy of this motion correction technique and its impact on quantitative tracer uptake measurements for simulated FDG-PET acquisitions. Furthermore, the method is extended to incorporate the obtained motion information directly into the image reconstruction of both MR and PET data.

METHODS: MR image acquisition: MR data was acquired with a bit-reversed radial phase encoding (RPE) trajectory which yields both high resolution 3D anatomical images and dynamic images with arbitrary temporal resolution. This sampling scheme was implemented on a 3T MRI scanner (Philips Healthcare). In 3 volunteers T1w GRE (FA 7°, TR/TE 6/3ms, 4min) and T2w TSE (FA 90°/120°, TR/TE 365/7.1ms, 7min) data were acquired: 288mm^3 FOV, 1.5mm^3 isotropic resolution. During data acquisition volunteers were advised to carry out 2-3 bulk motion shifts which led to sever motion artefacts (Fig 1). A pencil beam navigator was used to minimise respiratory motion artefacts.

PET simulation: PET simulations were carried out using STIR [6] based on segmented MR Dixon images which were acquired in addition to the T1w and T2w images. Virtual lesions (diameters: 7.5 - 19.5mm) were placed manually at accurately determined anatomical landmarks for each bulk motion state.

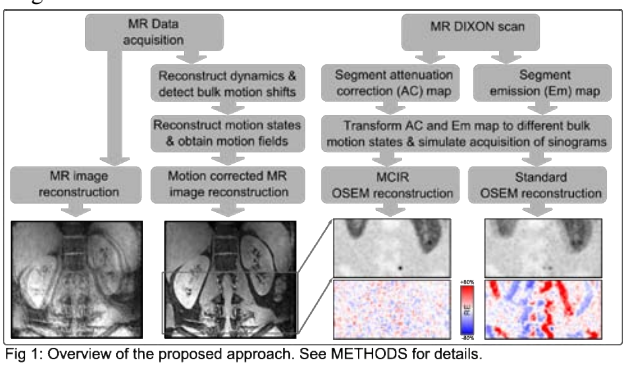

Fig 1: Overview of the proposed approach. See METHODS for details.

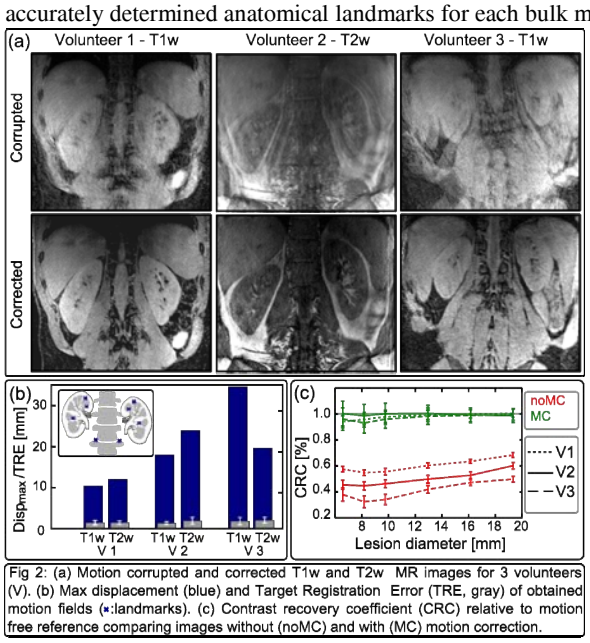

Fig 2: (a) Motion corrupted and corrected T1w and T2w MR images for 3 volunteers (V). (b) Max displacement (blue) and Target Registration Error (TRE, gray) of obtained motion fields (•:landmarks). (c) Contrast recovery coefficient (CRC) relative to motion free reference comparing images without (noMC) and with (MC) motion correction.

Bulk motion detection and correction: In a first step the recorded data are split into 55 dynamic time frames with a high temporal resolution. Images are reconstructed from this dynamic data to detect when bulk motion occurred using a global affine registration algorithm [8]. Since image quality is low, the dynamics are only used for bulk motion detection. Secondly, images describing each bulk motion state are reconstructed. More data is used for this reconstruction hence the image quality is high enough to estimate non-rigid motion between each bulk motion state. All images were reconstructed using a non-Cartesian iterative SENSE reconstruction [9]. The obtained motion information was incorporated into a motion compensated PET (MCIR with ordered subsets expectation maximization (OSEM), 23 subsets, 2 full iterations) and MR image reconstruction to obtain the best image quality possible [7,10] .

Accuracy of motion correction and assessment of tracer uptake: A 3D target registration error (TRE) was calculated at 8 landmark points which were manually selected for all bulk motion states (Fig 2b). The relative error (RE) between motion free reference (MF), motion corrupted (noMC) and motion corrected (MC) images was calculated as the pixel wise relative difference in SUV (red/blue images in Fig 1). The contrast recovery coefficient (CRC) was determined as the measured SUV of a lesion relative to the background signal of the surrounding tissue.

RESULTS: Every bulk motion shift in any of the 6 data sets could be accurately detected and corrected. The maximum displacement of the landmarks ranged from 10 to 30mm. With our approach this displacement could be reduced to a TRE of 1.71 ± 0.29mm. Bulk motion shifts led to a severe underestimation of SUV with smaller lesions affected more strongly with errors larger than 65% which were reduced to below 10% using the motion compensated reconstruction approach.

CONCLUSION: We have presented a technique which detects and corrects for non-rigid bulk motion shifts with an accuracy of 1.71 ± 0.29mm. In addition, the obtained bulk motion fields were used to successfully compensate for the same bulk motion in a simulated simultaneous PET-MR acquisition. The results of our PET simulation suggest that bulk motion can lead to an error in SUV assessment of up to 67%. Compensating the PET data for motion reduced this error to below 10% compared to a motion free reference. The presented results emphasise the importance to correct even for small motion and shows the potential of simultaneous PET-MR to ensure an accurate quantitative PET assessment. RPE is a highly flexible sampling scheme yielding both motion information and multi-contrast image information with high isotropic resolution. This makes this sampling scheme perfectly suited for simultaneous PET-MR acquisitions providing a wide range of MR information without increasing the overall scan time.

REFERENCES: [1] Bohmanji *et al.*, Lancet Oncol, 2001:2:157-64. [2] Young *et al.*, Eur J Cancer, 1999:35:1773-82. [3] Nehmeh *et al.*, Med Phys, 2002:29:366-37. [4] Gaa *et al.*, Eur J Med Res, 2004:9:309-12. [5] Judenhofer *et al.*, Nat Med, 2008:14:459-65. [6] Kolbitsch *et al.*, ISMRM, 2013:3745. [7] Tsoumpas *et al.*, Phys Med Bio, 2011:56:6597-613. [8] Buerger *et al.*, IEEE TMI, 2012:31:805-15. [9] Pruessmann *et al.*, MRM, 2001:46:638-651. [10] Batchelor et al., MRM, 2005:54:1273-80.